

Low-density series expansions for directed percolation: IV. Temporal disorder

Iwan Jensen

ARC Centre of Excellence for Mathematics and Statistics of Complex Systems, Department of Mathematics and Statistics, The University of Melbourne, Victoria 3010, Australia

E-mail: I.Jensen@ms.unimelb.edu.au

Received 22 October 2004

Published 2 February 2005

Online at stacks.iop.org/JPhysA/38/1441

Abstract

We introduce a model for temporally disordered directed percolation in which the probability of spreading from a vertex (t, x) , where t is the time and x is the spatial coordinate, is independent of x but depends on t . Using a very efficient algorithm we calculate low-density series for bond percolation on the directed square lattice. Analysis of the series yields estimates for the critical point p_c and various critical exponents which are consistent with a continuous change of the critical parameters as the strength of the disorder is increased.

PACS numbers: 05.50.+q, 05.10.–a

1. Introduction

Directed percolation (DP) can be thought of simply as a percolation process on a directed lattice in which connections are allowed only in a preferred direction, e.g., on hyper-cubic lattices connections are only allowed along edges connecting vertices with increasing coordinates. DP is most commonly interpreted as a growth model and the preferred direction t is time. Bond percolation is also a special case of a $(d + 1)$ -dimensional stochastic cellular automaton [4]. On the square lattice the evolution is governed by the transition probabilities $W(\sigma_x | \sigma_l, \sigma_r)$, with $\sigma_i = 1$ if the vertex i is occupied and 0 otherwise, which is the probability of finding the vertex x in state σ_x at time t given that, at time $t - 1$, the vertices $x - 1$ and $x + 1$ were in states σ_l and σ_r , respectively. Bond percolation corresponds to the choice $W(0 | \sigma_l, \sigma_r) = (1 - p)^{\sigma_l + \sigma_r}$. The behaviour of the model is controlled by the spreading probability (or density of bonds) p . When p is smaller than a critical value p_c all clusters remain finite, and in this sub-critical region any initial population will eventually die out. Above p_c there is a non-zero probability of finding an infinite cluster, the average cluster-size $S(p)$ diverges as $p \rightarrow p_c$, and the initial population will increase exponentially fast.

Directed percolation, and a closely related continuous time version the contact process [9], serve as the prime examples of models for population growth exhibiting a non-equilibrium

phase transition into an absorbing state (a state from which the system cannot escape), in these cases the state totally devoid of occupied sites. DP-type transitions are also encountered in many other situations, perhaps most prominently in models for chemical reactions [21, 6] including heterogeneous catalysis and surface reactions [22]. For a recent comprehensive review see [10].

Most studies of non-equilibrium systems have been limited to cases without disorder, that is the spreading probability is homogeneous in both time and space. Obviously in many real systems this idealization is unrealistic. Often some degree of disorder is present, e.g., in a real catalyst some sites may be blocked by impurities leading one to consider models with quenched spatial disorder. Likewise in trying to model real growth processes one would like to consider temporal disorder so as to model changes in conditions from year to year, seasonal changes, etc.

Non-equilibrium models with quenched spatial disorder were considered by Kinzel [17]. He argued that the Harris criterion [8], well known from disordered spin systems, should apply for DP as well. Harris argued that in systems with quenched disorder one must have $d\nu \geq 2$, where ν is the correlation length exponent. This means that quenched disorder is a relevant perturbation and thus should change the critical exponents if in the pure system $d\nu < 2$. The Harris criterion has been rigorously established for a large class of disordered systems by Chayes *et al* [2]. In the case of DP the Harris criterion becomes $d\nu_{\perp} < 2$, and quenched disorder is a relevant perturbation for $d \leq 3$. The effect of quenched disorder was studied numerically by Noest [19, 20] who found a marked change in the static critical exponents independent of the strength of the disorder. Moreira and Dickman [18, 3] used Monte Carlo simulations to study the site-diluted two-dimensional contact process on the square lattice. They found a marked change in the static critical exponents β and ν_{\perp} with a value of $\nu_{\perp} = 1.00(9)$ consistent with the Harris criterion. The dynamic behaviour was found to be incompatible with the usual scaling observed in pure models. In particular, critical spreading was found to be logarithmic rather than power law, and the survival probability in the sub-critical regime decayed algebraically rather than exponentially. This means that the dynamical critical correlation length exponent ν_{\parallel} is undefined. Janssen [13] investigated the problem using renormalization group theory and confirmed the findings of Moreira and Dickman. Recently, Hooyberghs, Iglói and Vanderzande [11, 12] have investigated these problems using a real-space renormalization group framework and the numerical technique of the density matrix renormalization group. They found that for strong enough disorder the behaviour is controlled by a strong disorder fixed point, with logarithmic dynamical correlations and critical exponents different from the pure system. For weaker disorder the numerical evidence was consistent with continuously varying static exponents.

Kinzel [17] also briefly considered the effect of temporal disorder and argued that a Harris-type criterion applied but with $d\nu_{\perp}$ replaced with ν_{\parallel} . Since $\nu_{\parallel} = 1.733\,847(6)$ [16] for (1+1)-dimensional DP this would make temporal disorder a relevant perturbation. In a previous paper [15], we studied temporally disordered directed percolation on the square lattice using a simple model in which spreading from some rows was *deterministic* (that is spreading takes place with probability 1) while spreading from the other rows took place with probability p as in the pure model. Disorder was introduced by letting any given row be ‘deterministic’ with probability α independent of other rows. The model was studied using high-density series expansions for the percolation probability and Monte Carlo simulations of growing clusters from a single seed. The major finding was that the critical exponents changed continuously with the strength of the disorder. In particular, we found that $\nu_{\parallel} < 2$ over a wide range of values in apparent violation of the Harris criterion.

The model used in [15] is not suitable for a low-density expansion so in this paper we study another model of DP with temporal disorder. The spreading probability $p(t)$ is chosen at random to be either p or αp with probability $\frac{1}{2}$. By varying the parameter α we can vary the strength of the disorder. There is an obvious symmetry between the two regions $\alpha < 1$ and $\alpha > 1$ and we shall therefore only consider the case $\alpha > 1$. Analysis of the series indicate that for any given value of α there is critical point $p_c(\alpha)$ where the system has a phase transition. For values of the spreading probability p close to $p_c(\alpha)$ the model changes from periods of sub-critical to periods of super-critical growth. For large values of α there is a very pronounced difference between the two regimes and the population dynamics changes from feast to famine. In the infinite lattice limit the system will have arbitrarily long stretches of ‘famine’ conditions in which the population is rapidly reduced and very likely do die out. Note that we can be sure that the model will have sub- and super-critical regions. We can simply choose $p > p_c$, where p_c is the critical point of the pure model, and we will always have a super-critical growth process, while for $\alpha p < p_c$ the growth process is always sub-critical.

In section 2, we give a description of the method used to derive the low-density series for this model. The series is then analysed (for various values of α) and the results are presented in section 3. Finally, section 4 contains a brief summary and discussion of the main results.

2. Calculation of low-density series

In the low-density phase ($p < p_c$) many quantities of interest can be derived from the pair-connectedness $C_{t,x}(p)$, which is the probability that the vertex at position x is occupied at time t given that the origin was occupied at $t = 0$. Of particular interest are moments of the pair-connectedness

$$\mu_{m,n}(p) = \sum_t \sum_x t^m x^n C_{t,x}(p). \tag{1}$$

Due to symmetry moments involving odd powers of x are identically zero. The remaining moments diverge as p approaches p_c from below

$$\mu_{m,n}(p) \propto (p_c - p)^{-(\gamma + m\nu_{\parallel} + n\nu_{\perp})}, \quad p \rightarrow p_c^- \tag{2}$$

In a previous paper [16], we gave a detailed description of how the graph theoretical properties of the pair-connectedness [1] can be turned into a very efficient algorithm for the calculation of low-density series expansions for ordinary directed percolation. The series expansions for the disordered model is a simple generalization of this work. Before describing the algorithm for the disorder system we will briefly review the pure case.

It has been shown [1] that the pair-connectedness can be expressed as a sum over all graphs (or finite clusters) formed by taking unions of directed paths connecting the origin to the vertex (x, t) ,

$$C_{t,x}(p) = \sum_g d(g) p^{|g|}, \tag{3}$$

where $|g|$ is the number of bonds in g . The weight $d(g) = (-1)^{c(g)}$, where $c(g)$ is the cyclomatic number of the graph g . Note that $c(g)$ is increased by 1 whenever two paths join, e.g., if there are two incoming bonds on a vertex. The restriction to unions of paths is very strong and one immediate consequence is that graphs with dangling parts make no contribution to $C_{t,x}$ and any contributing graph terminates exactly at (t, x) . Another way of stating the restriction is that any vertex with an incoming bond *must* have an outgoing bond unless it is the terminal vertex (t, x) . Any directed path to a vertex whose parallel distance from the origin is t contains at least t bonds. One can do much better by using a

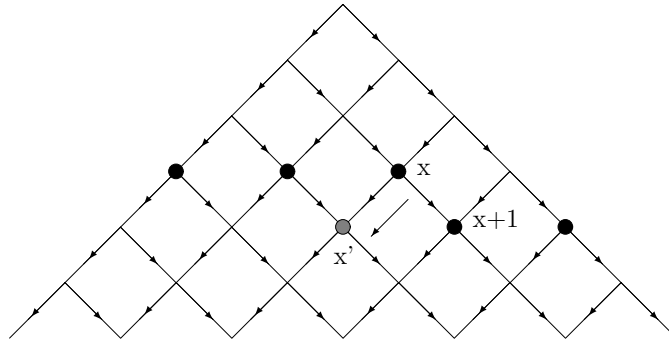


Figure 1. Example of how the boundary line (cutting through the filled circles) is moved in order to insert another vertex (shaded circle).

so-called non-nodal graph expansion [5] to extend the series to order $2t$. A graph g is nodal if it has a vertex (other than the terminal vertex) through which all paths pass. It is clear that each such nodal point effectively works as a new origin for the cluster growth, and we can obviously obtain any contributing graph by concatenating non-nodal graphs. Note that the graph consisting of a single bond is non-nodal so all linear graphs can be obtained by repeated concatenations. This is the essential idea behind the non-nodal graph expansion, which proceeds in two principal steps. First, we calculate the contribution $C_{t,x}^*$ of non-nodal graphs to the pair-connectedness. The calculation is done up to a preset order N , where N is limited by the available computational resources (primarily physical memory). Next, we use repeated concatenation operations of $C_{t,x}^*$ to calculate the pair-connectedness $C_{t,x}$ and from this we finally calculate various moments $\mu_{m,n}(p)$.

The calculation of $C_{t,x}^*$ is done efficiently using transfer-matrix techniques. This involves drawing a boundary line across a finite slice of the lattice and then moving the boundary line such that one adds row after row with each row built up one vertex at a time, as illustrated in figure 1. The sum over all contributing graphs is calculated as the lattice is constructed. At any given stage the boundary line cuts through a number of, say j , vertices. There are two possible states (0 or 1) per vertex, corresponding to vertices with (1) or without (0) incoming bonds, leading to a total of 2^j possible boundary configurations. However, as explained in [16] not all the 2^j possible configurations are required. Many of them can be discarded because they either do not make a contribution to $C_{t,x}^*$ or only contributes above order N . The weight of each configuration is given by a polynomial P in p truncated at order N . The updating of P , as the boundary line is moved to insert a new vertex, depends only on the states of the vertices marked x and $x + 1$ in figure 1 and are given simply by

$$\begin{aligned}
 P(\bar{S}_{1,1}) &= p^2 P(S_{1,0}) + pP(S_{1,1}) - p^2 P(S_{1,1}), \\
 P(\bar{S}_{0,1}) &= pP(S_{1,0}) + P(S_{0,1}) - pP(S_{1,1}), \\
 P(\bar{S}_{1,0}) &= pP(S_{1,0}), \\
 P(\bar{S}_{0,0}) &= P(S_{0,0}).
 \end{aligned}
 \tag{4}$$

Here $S_{a,b}$ is the configuration before the move which has the vertex at x in state a and the vertex at $x + 1$ in state b , while $\bar{S}_{a,b}$ is the configuration after the move which has the new vertex at x' in state a and the vertex at $x + 1$ in state b . For a derivation of the updating rules see [16].

Limiting the calculation to non-nodal contributions is very simple; whenever the boundary line reaches the horizontal position one just sets to zero the polynomials of states with a single incoming bond. This obviously ensures that configurations with a nodal point are deleted from the calculation. The pair-connectedness at the following time can be calculated from the states with incoming bonds at nearest-neighbour sites and no incoming bonds on any other sites. In this way, we calculate the two non-nodal series $C_t^*(p) = \sum_x C_{t,x}^*(p)$ and $X_t^*(p) = \sum_x x^2 C_{t,x}^*(p)$.

The generalization to DP with temporal disorder is quite simple. First of all the configuration weights P will depend on two variables u and v corresponding to the two spreading probabilities. Let us consider the situation in which a row has just been completed. Since the probability is $\frac{1}{2}$ that spreading from a given row occurs with probability u or v , respectively, obviously $\bar{P}(u, v) = P(v, u)$. Next, we insert a new row. Formally, we can express the weight of any new configuration \bar{S} as a weighted sum over the weights of the configurations S in the row above

$$P_{\bar{S}}(u, v) = \sum_S W(u) P_S(u, v) + \sum_S W(v) P_S(u, v). \tag{5}$$

From the nature of the problem it is clear that the weight W is the same (apart from the change of variable). This means that it is very simple to calculate the non-nodal expansion. Having completed a row, we just use the updating rules in equation (4) with the spreading fixed at u . This gives a set of incomplete weights

$$Q_{\bar{S}}(u, v) = \sum_S W(u) P_S(u, v). \tag{6}$$

But since $P_S(u, v)$ is symmetric in u and v we get the desired final result as

$$P_{\bar{S}}(u, v) = Q_{\bar{S}}(u, v) + Q_{\bar{S}}(v, u). \tag{7}$$

Note that this is a very efficient algorithm. Naively one would have expected that to calculate the pair-connectedness one would have to sum over all 2^t realizations of the disorder. However, as we have just seen this is not necessary, the only complication being the requirement to maintain a two parameter generating function. Ultimately, we shall calculate series for $\mu_{m,n}(p)$, by fixing a value of α and setting $u = p$ and $v = \alpha p$. So we need to retain only the coefficients of $u^i v^j$ provided $i + j \leq N$. The first few terms in the expansion for $C_t^*(u, v)$ are

$$\begin{aligned} C_1^*(u, v) &= 2(u + v) \\ C_2^*(u, v) &= -u^4 - 2u^2v^2 - v^4 \\ C_3^*(u, v) &= 2u^7 - 2u^6 + (4u^5 - 6u^4)v^2 + 2u^4v^3 + (2u^3 - 6u^2)v^4 + 4u^2v^5 - 2v^6 + 2v^7 \\ C_4^*(u, v) &= u^{12} - 4u^{11} + 8u^9 - 5u^8 + (2u^{10} - 8u^9 + 24u^7 - 20u^6)v^2 - (4u^8 - 8u^6)v^3 \\ &\quad + (3u^8 - 8u^7 + 24u^5 - 30u^4)v^4 - (8u^6 - 24u^4)v^5 + (4u^6 - 8u^5 + 8u^3 - 20u^2)v^6 \\ &\quad - (8u^4 - 24u^2)v^7 + (4u^3 - 4u - 5)v^8 - (8u^2 - 8)v^9 + 2u^2v^{10} - 4v^{11} + v^{12}. \end{aligned}$$

Note that $C_t^*(p, p)$ is $2^t C_t^*(p)$, where $C_t^*(p)$ is the non-nodal pair-connectedness of the pure model. In order to calculate our final series for the average cluster-size $S(p)$ and the moments $\mu_{1,0}(p)$ and $\mu_{2,0}(p)$ we simply fix a value of α . We then use repeated concatenations of $C_t^*(p, \alpha p)/2^t$ to calculate the pair-connectedness $C_t(p)$ (with α fixed), which in turn we use to calculate the moments. The series for the second transverse moment $\mu_{0,2}$ is obtained as $\mu_{0,2} = S^2(p) \sum_t X_t^*(p)$.

The series for $C_t^*(u, v)$ was derived correctly to order 115 (that is all coefficients of $u^i v^j$ were calculated exactly for $i + j \leq 115$). This obviously results a series for $S(p)$ and the other moments to order 115 as well. The algorithm used up to 5 GB of physical memory and the total CPU time was about 30 days.

Table 1. Estimates for the critical point p_c and critical exponents γ , ν_{\parallel} and ν_{\perp} at various values of the disorder strength α .

α	p_c	γ	ν_{\parallel}	ν_{\perp}
1.00	0.644 7002(2)	2.277 65(5)	1.733 85(5)	1.096 87(1)
1.02	0.638 3905(5)	2.2779(1)	1.734 42(8)	1.097 45(5)
1.04	0.632 3450(10)	2.2825(5)	1.736 35(15)	1.0993(2)
1.06	0.626 5485(15)	2.2895(10)	1.7394(3)	1.1025(5)
1.08	0.620 9865(25)	2.299(2)	1.7435(5)	1.1068(10)
1.10	0.615 645(4)	2.310(5)	1.748(2)	1.1135(25)
1.20	0.591 83(3)	2.40(5)	1.785(10)	1.16(3)
1.30	0.572 00(6)	2.5(1)	1.825(25)	1.19(4)
1.40	0.555 20(10)	2.57(7)	1.875(50)	1.25(5)
1.50	0.5407(2)	2.7(1)	1.92(5)	1.33(10)
1.60	0.5282(4)	2.8(2)	1.95(8)	1.36(10)
1.70	0.5174(6)	2.9(2)	2.0(1)	1.34(10)

3. Analysis of series

The various series were analysed using inhomogeneous differential approximants [7]. Suffice to say that a K th-order differential approximant to a function f is a solution to an inhomogeneous differential equation

$$\sum_{i=0}^K Q_i(x) \left(x \frac{d}{dx} \right)^i \tilde{f}(x) = P(x), \quad (8)$$

where the coefficients in the polynomials Q_i and P of order N_i and L , respectively, are chosen so that the series for the function $\tilde{f}(x)$ agrees with the series coefficients of f . The equations are readily solved as long as the total number of unknown coefficients in the polynomials is smaller than the order of the series n . The possible singularities of the series appear as the zeros x_i of the polynomial Q_K and the associated critical exponent λ_i is estimated from the indicial equation.

Our use of differential approximants for series analysis has been detailed in previous papers [14, 16] and the interested reader can refer to these papers and the comprehensive review [7] for further details. Typically, we obtain estimates for p_c and the critical exponents by averaging values obtained from second- and third-order differential approximants. For each order L of the inhomogeneous polynomial we average over those approximants which use at least the first 90% of the terms in the series. A rough error estimate is obtained from the spread among the approximants. Note that these error bounds should *not* be viewed as a measure of the true error as they cannot include possible systematic sources of error.

In figure 2, we have plotted the estimates for the critical point p_c and the critical exponents γ , ν_{\parallel} and ν_{\perp} as a function of the disorder strength α (some of the estimates are listed explicitly in table 1). The estimates were obtained by analysing the series $S(p) \propto (p - p_c)^{-\gamma}$, $\mu_{2,0}(p)/\mu_{1,0}(p) \propto (p - p_c)^{-\nu_{\parallel}}$ and $\mu_{0,2}(p)/S(p) \propto (p - p_c)^{-2\nu_{\perp}}$, respectively, and are based on results using both second- and third-order differential approximants with varying degrees of the inhomogeneous polynomial. The results are clearly compatible with a continuous change in all the critical parameters as the strength of the disorder α increases. Naturally, we observe a decrease in the value of the critical point p_c , and in particular we note that $\alpha p_c \leq 1$. The critical exponents all increase with increasing α . In particular we note that $\nu_{\parallel} < 2$, at least when $\alpha \leq 1.5$. It is also clear that the change in the values of the critical

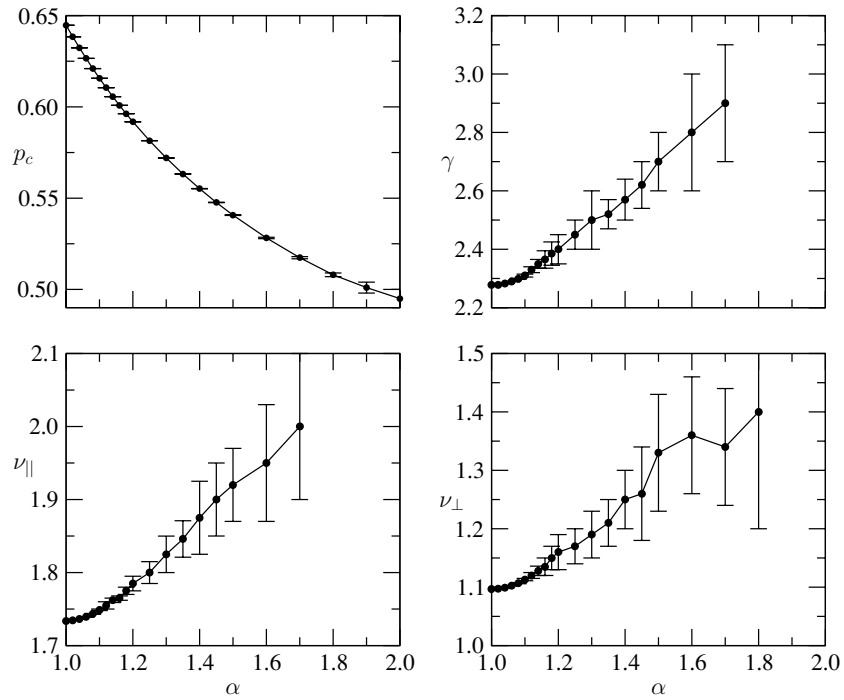


Figure 2. Estimates for the critical point p_c and critical exponents γ , ν_{\parallel} and ν_{\perp} as a function of the disorder strength α .

Table 2. Estimates of the critical point p_c and critical exponents γ , ν_{\parallel} and $2\nu_{\perp}$ with $\alpha = 1.1$, as obtained from third-order differential approximants (L is the order of the inhomogeneous term).

L	p_c	γ	p_c	ν_{\parallel}	p_c	$2\nu_{\perp}$
0	0.615 6457(10)	2.3114(29)	0.615 644(71)	1.83(11)	0.615 6455(42)	2.2275(43)
5	0.615 6454(17)	2.3115(17)	0.615 634(35)	1.765(23)	0.615 6474(25)	2.2294(29)
10	0.615 6399(16)	2.3070(15)	0.615 6464(23)	1.7489(11)	0.615 6449(28)	2.2268(29)
15	0.615 6437(22)	2.3101(18)	0.615 6427(82)	1.7491(30)	0.615 6458(28)	2.2277(30)
20	0.615 6460(26)	2.3121(25)	0.615 6407(85)	1.7483(26)	0.615 6447(79)	2.2270(75)

exponents is larger than the estimated error bars, clearly indicating that the change is not due merely to less well-behaved series. When the disorder is relatively weak (α close to 1) the estimates for both p_c and the exponents are still quite sharp, but as α is increased the estimated error bars become large and for values of $\alpha \geq 1.5$ the exponent estimates are inaccurate.

As a concrete example of the analysis we show some detailed results from the analysis with the particular value $\alpha = 1.1$. In table 2, we have listed estimates for p_c and the critical exponents γ , ν_{\parallel} and $2\nu_{\perp}$. The estimates of p_c are consistent to five digits both among the three series as well as among the approximants using different orders of the inhomogeneous polynomial. Likewise the estimates for the exponents are consistent as we vary the order of the inhomogeneous polynomial (the only exception being the $L = 0$ and $L = 5$ estimates of ν_{\parallel}). Taking into account the spread among the different sets of approximants (while ignoring the obviously spurious results for ν_{\parallel}) we arrive at the estimates listed in table 1. To gauge whether there are pronounced sources of systematic errors we plot in figure 3 the estimates for the

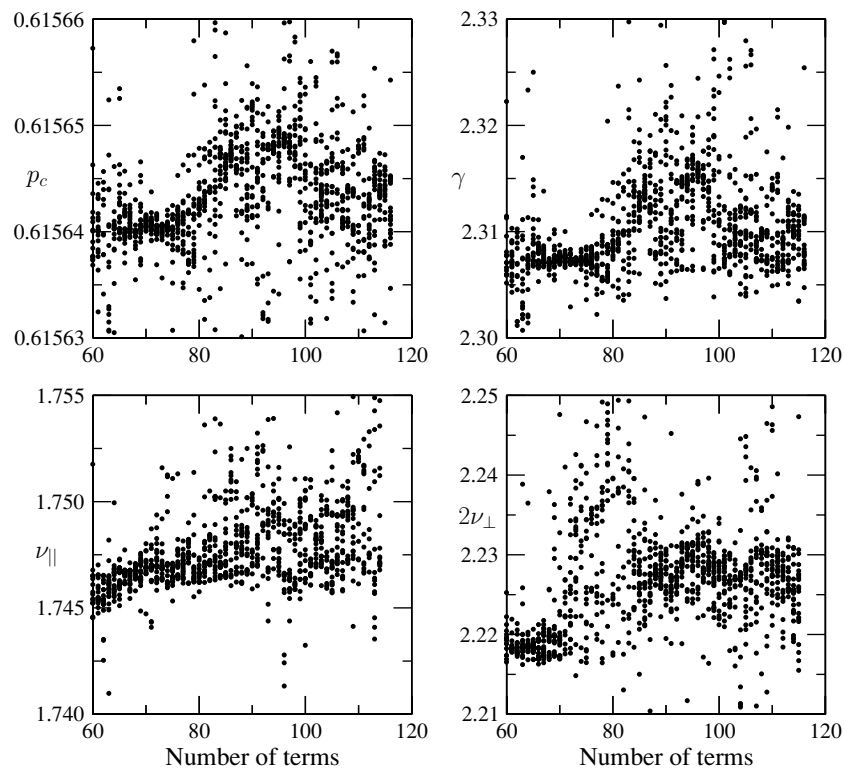


Figure 3. Estimates of the critical point p_c and critical exponents γ , ν_{\parallel} and $2\nu_{\perp}$ with $\alpha = 1.1$ plotted versus the number of terms used by the third-order differential approximants.

critical point p_c and the critical exponents γ , ν_{\parallel} and $2\nu_{\perp}$ as a function of the number of terms used by the differential approximants. The critical point estimates are those obtained from the cluster-size series $S(p)$. Each point in these plots corresponds to the estimate obtained from a single third-order differential approximant. From these plots we observe that the estimates do not change much as the number of terms is increased and thus conclude that there does not appear to be any systematic errors in the estimates.

4. Summary

We have introduced a simple model for directed percolation with temporal disorder, described a very efficient algorithm for the derivation of low-density series expansions for this model and presented results from the analysis of the series. The main result from the series analysis is that the model has a critical point $p_c(\alpha)$ which varies continuously with α as does the critical exponents γ , ν_{\parallel} and ν_{\perp} . The estimates for the critical exponent $\nu_{\parallel} < 2$ for most values of the disorder in apparent violation of the Harris criterion.

E-mail or WWW retrieval of series

The series for the directed percolation problem studied in this paper can be obtained via e-mail by sending a request to I.Jensen@ms.unimelb.edu.au or via the world wide web on the URL <http://www.ms.unimelb.edu.au/~iwan/> by following the relevant links.

Acknowledgments

The calculations presented in this paper were in part performed on the facilities of the Australian Partnership for Advanced Computing (APAC) and the Victorian Partnership for Advanced Computing (VPAC). We gratefully acknowledge financial support from the Australian Research Council.

References

- [1] Arrowsmith D K and Essam J W 1977 Percolation theory on directed graphs *J. Math. Phys.* **18** 235–8
- [2] Chayes J T, Chayes L, Fisher D S and Spencer T 1986 Finite-size scaling and correlation lengths for disordered systems *Phys. Rev. Lett.* **57** 2999–3002
- [3] Dickman R and Moreira A G 1998 Violation of scaling in the contact process with quenched disorder *Phys. Rev. E* **57** 1263–8
- [4] Domany E and Kinzel W 1984 Equivalence of cellular automata to Ising models and directed percolation *Phys. Rev. Lett.* **53** 311–4
- [5] Essam J W, Guttmann A G and De'Bell K 1988 On two-dimensional directed percolation *J. Phys. A: Math. Gen.* **21** 3815–32
- [6] Grassberger P and de la Torre A 1979 Reggeon field theory (Schlögl's first model) on a lattice; Monte Carlo calculations of critical behaviour *Ann. Phys., NY* **122** 373–96
- [7] Guttmann A J 1989 Asymptotic analysis of power-series expansions *Phase Transitions and Critical Phenomena* vol 13 ed C Domb and J L Lebowitz (New York: Academic) pp 1–234
- [8] Harris A B 1974 Effects of random defects on the critical behaviour of Ising models *J. Phys.: Condens. Matter* **7** 1671–92
- [9] Harris T E 1974 Contact interactions on a lattice *Ann. Prob.* **2** 969–88
- [10] Hinrichsen H 2000 Non-equilibrium critical phenomena and phase transitions into absorbing states *Adv. Phys.* **49** 815–958
- [11] Hooyberghs J, Iglói F and Vanderzande C 2003 Strong disorder fixed point in absorbing-state phase transitions *Phys. Rev. Lett.* **90** 100601
- [12] Hooyberghs J, Iglói F and Vanderzande C 2004 Absorbing state phase transitions with quenched disorder *Phys. Rev. E* **69** 066104
- [13] Janssen H K 1997 Renormalized field theory of the Gribov process with quenched disorder *Phys. Rev. E* **55** 6253–6
- [14] Jensen I 1996 Low-density series expansions for directed percolation on square and triangular lattices *J. Phys. A: Math. Gen.* **29** 7013–40
- [15] Jensen I 1996 Temporally disordered bond percolation on the directed square lattice *Phys. Rev. Lett.* **77** 4988–91
- [16] Jensen I 1999 Low-density series expansions for directed percolation: I. A new efficient algorithm with applications to the square lattice *J. Phys. A: Math. Gen.* **32** 5233–49
- [17] Kinzel W 1985 Phase transitions of cellular automata *Z. Phys. B* **58** 229–44
- [18] Moreira A G and Dickman R 1996 Critical dynamics of the contact process with quenched disorder *Phys. Rev. E* **54** R3090–3
- [19] Noest A J 1986 New universality for spatially disordered cellular automata and directed percolation *Phys. Rev. Lett.* **57** 90–3
- [20] Noest A J 1988 Power-law relaxation of spatially disordered stochastic cellular automata and directed percolation *Phys. Rev. B* **38** 2715–20
- [21] Schlögl F 1972 Chemical reaction models for non-equilibrium phase transitions *Z. Phys.* **252** 147–61
- [22] Ziff R M, Gulari E and Barshad Y 1986 Kinetic phase transitions in an irreversible surface-reaction model *Phys. Rev. Lett.* **56** 2553–6